Experimental investigation on DMFCs using reduced noble metal loading with NiTiO3 as supportive material to enhance cell performances

Experimental Investigation on DMFCs Using Reduced Noble Metal Loading with $NiTiO_3$ as Supportive Material to Enhance Cell Performances

Thiagarajan V[a]; Karthikeyan P*[a]; Thanarajan K[a]; Neelakrishnan S[a]; Manoharan R[b]; Rui Chen[c]; Ashley Fly[c]; Anand R[d]; Thundil R Karuppa Raj[e];

Sendhil Kumar N[f];

a: Fuel Cells and Energy Systems Laboratory, Department of Automobile Engineering, PSG College of Technology, Coimbatore-641004, India

b: Door No. 6, 3rd Street, Mahalakshmi Nagar, K. K Nagar, Tiruchirappalli, 620021, India

c: Department of Aeronautical and Automotive Engineering, Loughborough University, Loughborough, United Kingdom

d: Department of Mechanical Engineering, National Institute of Technology (NIT), Tiruchirappalli, India

e: School of Mechanical Engineering, Vellore Institute of Technology, Vellore, India

f: Department of Mechanical Engineering, National Institute of Technology (NIT Puducherry), Karaikal, India

**Corresponding Author: P. Karthikeyan, Professor, Fuel Cells and Energy Systems Laboratory, Department of Automobile Engineering, PSG College of Technology, Coimbatore - 641004, India.Tel.: +91- 422-2572177; Fax: +91- 422-2573833; Email address: apkarthipsg@gmail.com; apk.auto@psgtech.ac.in*

Abstract

In this present work, the effect of anode electrocatalyst materials is investigated by adding $NiTiO_3$ with Pt/C and Pt-Ru/C for the performance enhancement of direct methanol fuel cells (DMFCs). The supportive material $NiTiO_3$/C has been synthesized first by wet chemical method followed by incorporation of Pt and Pt-Ru separately. Experiments are conducted with the combination of four different electrocatalyst materials on **the** anode side (Pt/C, Pt-$NiTiO_3$/C, PtRu/C, Pt-Ru-$NiTiO_3$/C) and with commercial 20 wt. % Pt/C on the cathode side; 0.5 mg_{pt}/cm^2 loading is maintained on both sides. The performance tests of the above catalysts are conducted on 5 cm^2 active area with various operating conditions like cell operating temperatures, methanol/water molar concentrations and reactant flow rates. Best performing operating conditions have been optimized. The maximum peak power densities attained are 13.30 mW/cm^2 (26.6 mW/mg_{pt}) and 14.60 mW/cm^2 (29.2 mW/mg_{pt}) for Pt-$NiTiO_3$/C and Pt-Ru-$NiTiO_3$/C at 80 ℃, respectively, with 0.5 M concentration of methanol and fuel flow rate of 3 ml/min (anode) and oxygen flow rate of 100 ml/min (cathode). Besides, 5 h short term stability tests have been conducted for PtRu/C and Pt-$NiTiO_3$/C. The overall results suggest that the incorporation of $NiTiO_3$/C supportive material to Pt and Pt-Ru appears to make a promising anode electrocatalysts for the enhanced DMFC performances.

Keywords: Direct Methanol Fuel Cell, Anode Electrocatalyst, Nickel Titanate, Methanol oxidation, Cell Performance.

1. Introduction

Due to the depletion of fossil fuel and the increase in global warming, an alternative energy source was required to fulfil the energy requirements. **The** fuel cell is regarded as one of the most promising alternate energy producing devices to meet the energy requirements. Many types of fuel cells are available in the market such as Proton Exchange Membrane Fuel Cell (PEMFC), Solid Oxide Fuel Cell (SOFC), Molten Carbonate Fuel Cell (MCFC), Alkaline Fuel Cell (AFC) and Phosphoric Acid Fuel Cell (PAFC) for various targeted applications. Among different types, Direct Methanol Fuel Cell (DMFC) is chosen as our thrust area is high, due to its operating temperature, high energy density, **high conversion efficiency at ambient operating conditions** and energy offered by methanol when compared with hydrogen [1-3]. The DMFCs have been identified as the promising power source to compete with conventional batteries for powering portable electronic devices as it does not require any fuel processing unit and easy to transport and storage [4,5]. However**, the** performance of anodic side of the DMFCs still remains a challenge due to issues like, methanol crossover, higher level loading of Pt on the electrodes, **low dynamics of methanol reaction rates (electrooxidation)** and catalyst poisoning due to **the** formation of CO [6-**8**]. In order to overcome these challenges, an effort has been made to reduce methanol crossover and membrane swelling by decreasing the methanol concentration and increasing the thicknesses of the membrane and Gas Diffusion Layer (GDL) [9,10]. Still, optimization of operating temperature and effective catalyst material are required to enhance the chemical reaction rate of DMFCs. On the other hand, in order to reduce the CO poisoning and effective conversation of CO to CO_2 adsorbed on the layer of catalyst, a catalytic material or higher amount of catalyst loading is requird [11]. Several numerical and experimental studies have been conducted for the synthesis of catalyst materials, ink preparation, Membrane Electrode Assembly (MEA) fabrication and operating parameters to improve the performance of the

DMFC [12-18]. It is well understood that the performance of the DMFCs are greatly dependent on the anode catalyst material, which should have high activity, stability and durability. In this direction, many research investigations have been focused on selection and synthesis of catalysts materials to enhance the methanol oxidation reaction (MOR) activity [19-22], Platinum based electrocatalysts are highly used for fuel cells, however their poor tolerance towards CO hampers its activity. Therefore, Ruthenium was additionally incorporated into platinum as a strategy to reduce CO poisoning of catalyst and to effectively promote conversion of CO to CO_2 in the DMFCs [23-26]. Still, poor performance, electrocatalytic activity and durability are considered as the major problem in Pt-Ru composites. To overcome these issues, incorporation of non-noble metals or metal oxides with the anode electrocatalyst are often recommended to oxidize CO to CO_2 **which** improves the MOR activity and reduces **the Pt poisoning effect** [27-**29**], which is capable of absorbing oxygenated species with low loading of platinum (<0.5 mg/cm^2) [27].

Various research groups have demonstrated the incorporation of some of **the** metal oxides (TiO_2, IrO_2, CeO_2, V_2O_5, WO_x, MoO_3, $NiTiO_3$) as active support material in the anode electrocatalysts for the improvement of the MOR activity in the DMFCs [30-37]. In this aspect, TiO_2 has been recognized as one of the promising MOR reaction promoters with high stability under acidic environment. Additionally, due to the reduction of TiO_2 into Ti^{3+}, the electronic density of Pt has been altered and the bond between Pt and CO becomes weaker, **thus improves the MOR activity of Pt-based electrocatalyst by Tian X et.al [38]**. This helps to increase the ability of removing CO adsorbed on the surface of Pt [39]. During the MOR reaction, TiO_2 improves adsorption of OH species, and increases the conversion of poisonous CO to CO_2. Kang et al [40] showed that the MOR activity of the catalyst and performance of the electrode with $Pt_{0.5}$-$Ru_{0.4}$ M (M = Ni, Sn,and Mo) alloy catalyst was higher than Pt-Ru. Recently, we showed [37,41] that the presence of $NiTiO_3$ added with Pt/C

and PtRu/C (the alloy with the particular composition $Pt_{0.7}Ru_{0.3}$) promotes the anodic MOR activity and catalysts durability. We also proposed that such higher electrocatlytic activity is due to the promotional effect exhibited by surface Ru oxide and $NiTiO_3$.

In the present work, the performance of a 5 cm^2 active area DMFCs **was** assembled utilizing our novel catalyst materials for anodes and commercial Pt/C as the cathode catalyst and investigated experimentally. The platinum loading is maintained at 0.5 mg_{pt}/cm^2 for the catalysts Pt/C, Pt-$NiTiO_3$/C, PtRu/C, Pt-Ru-$NiTiO_3$/C. A series of experiments have been conducted to test the performances of the DMFCs under operating temperatures (45 ℃, 60 ℃, and 80 ℃), methanol molar concentrations (0.5 M, 1.0 M, 2.0 M and 3.0 M) and various flow rates on anode (1 ml/min, 2 ml/min, 3 ml/min and 4 ml/min) and cathode flow rate remains constant (100 ml/min). State of art of comparison of performances with other DMFC electrocatalysts **has** also been carried out for easy understandings. To the best of the author's knowledge, the performance of a 5 cm^2 active area DMFC with **a** low platinum loading of 0.5 mg_{pt}/cm^2 on Pt-$NiTiO_3$/C and Pt-Ru-$NiTiO_3$/C anode catalysts along with the influence of operating conditions has been studied.

2. Experimental

2.1 Synthesis and materials characterization

The following reagents and chemicals are used for material synthesis. Dihydrogenhexachloroplatinate (IV) hexahydrate ($H_2PtCl_6 \cdot 6H_2O$), methanol, isopropanol (Hi-Media), KOH, nickel acetate, titanium (IV) isopropoxide and citric Acid, Vulcan carbon XC-72, 5 wt. % **of** Nafion ionomer were purchased. The commercial Pt/C (Fuel cells Etc, USA) (20 wt.% Platinum and 80 wt.% on XC-72) is used as the cathode. The anode materials Pt/C, Pt-$NiTiO_3$/C, PtRu/C, Pt-Ru-$NiTiO_3$/C were synthesised using wet chemical method is Fig. S1. The atomic composition in Pt-Ru alloys is $Pt_{0.7}$ $Ru_{0.3}$. The weight percentage of the catalysts in all these materials is kept as 20 % and that of $NiTiO_3$ is also kept as 20 % in the

later materials. The phase formations of the synthesised materials have been confirmed by X-Ray Diffraction (XRD) using Philips X-ray diffractometer with Cu Kα radiation source. The morphologies of the catalysts have been investigated by TEM images by in a JEOL JEM 2100 equipment. The chemical bonding states have been evaluated by X-ray Photoelectron Spectroscopy (XPS) measurements using a PHI-5702 multifunctional Omicron Nanotechnology spectrometer, with Al Kα - radiation (1486.6 eV). The synthetic procedures, characterization results and the details of data anlysis have already been reported in our previous publications [37,41], **additionally Scanning Electron Microscope (SEM) characterization on the surface morphology using SEM Hitachi TM3030Plus equipment fitted with an OXFORD INSTRUMENTS swift ED3000 allowing Energy Dispersive X-ray Spectrometry (EDS) meaurements on catalyst layer (CL) are shown in Fig. S2.**

2.2 Catalyst ink preparation

The catalyst ink was prepared for all the catalyst powders using Nafion ionomer (taken from 10 wt. % of Nafion solution, Sigma Aldrich), isopropyl alcohol and deionized water used as a solvent [37]. Initially 20 mg of catalyst powder was weighed and put into the container followed by the addition of deionized water in the mass ratio 20:1, 5 wt. % of Nafion solution (60 µL) and isopropyl alcohol were used for making the catalyst ink in the concentration of 0.0252 mg/µL by adding more amount of isopropyl alcohol. The catalyst ink mixture was stirred by using Elmasonic S 30H ultrasonic bath having an ultrasonic frequency of 37 kHz with an effective ultrasonic power of ~80 W and homogenized for 120 minutes [42,43]. The temperature was maintained at 25 °C during homogenization of the catalyst ink.

2.3 Coating of catalyst ink on Gas Diffusion Layer (GDL)

Different methods exist for coating of catalyst ink onto the GDL: hand painting, rolling, spraying, and screen printing [44-46]. In-Su Park et al. [47] studied the catalyst slurry

coated on both sides of a Nafion membrane by doctor blade method for the mass production of high-quality MEAs. **Glass DE [48] et.al, described that the Doctor blade method consists of spreading a fine, uniform layer of catalyst ink onto the surface of GDL with multiple layers of equal thicknesses.** By using the doctor blade method in our work, the catalyst inks (Pt/C, Pt-$NiTiO_3$/C, PtRu/C and Pt-Ru-$NiTiO_3$/C) were coated on 5 cm^2 of gas diffusion carbon paper (GDL Toray, E-TEK) having the thickness of 370 μm. In this method, a smooth glass was used as a support for the substrate. Initialy, 5 cm^2 GDL was placed on the glass substrate, and 24.6 mg of catalyst ink (same amount used for all the catalysts) was dropped on GDL in front of the blade using a micropipette (Eppendrof Research Plus). The blade spreader with a height was driven through the catalyst ink until the coat covered a sufficient area of 5 cm^2 GDL. The volume of the catalyst ink, blade height, and drive speed were all adjusted for a catalyst ink composition until the desired 0.5 mg_{Pt}/cm^2 loading **was** achieved. The catalyst loading was determined by dry weight difference method of before and after **the** coating of **the** gas diffusion layer. The coated GDLs were dried in an oven at 30 ℃ for 1 h under the nitrogen atmosphere in order to remove any other oxides formation on the surface of the catalyst layer. Novel catalysts coated GDLs thus prepared were used for the fabrication of MEAs.

2.4 Pre-treatment of Nafion membrane and MEA fabrication

Nafion 117 membrane was used for all the MEAs, prior to fabrication of the membrane was treated to increase the activity of sulfonic groups and improve proton conductivity using the following steps [45]:

i. The Nafion membrane is soaked in 3 % H_2O_2 for an hour at 80 ℃.
ii. Then the membrane is soaked in deionized water for two hours at 80 ℃.
iii. The membrane again is soaked in 0.5 % H_2SO_4 solution for one hour at **the** same temperature.

iv. Finally, the membrane is rinsed with deionized water and stored in a beaker filled with deionized water, otherwise drying of the membrane leads to poor ionic conductivity.

The required size of Nafion 117 membrane was taken out and it was sandwiched between the catalyst coated anode GDL of 5 cm^2 active area and respective commercial Pt/C GDE. The whole thing was wrapped with Teflon sheet and placed in a hot press (Orione, India) at **120 °C under 50 kg/cm^2 pressure for 3 minutes. In general cell power density is strongly influenced by the fabrication conditions of the MEA along with associated cell components [49].**

2.5 DMFC Test Setup and Performance Measurements

The performances of single cells were evaluated by using 850e fuel cell test station (Scribner Associates, USA) which can be programmed to control accurately the electronic load (0-5 A), temperature (30 ^oC - 120 ^oC), oxidant flow rate (1 ml/min to 2000 ml/min) and relative humidity of the reactants (0-100%). The fuel cell test system is interfaced to a computer system using Fuel Cell 4.3h software package. The acquisition of data is achieved by using FuelCell software with GPIB interface. The capability of **the** fuel cell test station is upto 100 W power with maximum voltage and current of 20 V and 5 A respectively. The cathode flow rate was controlled by a mass flow meter in Scribner test station and in anode, the methanol flow rate was controlled by an external peristaltic pump (Master Flex, USA) interfaced with Scribner test setup with minimum and maximum flow rates of 0.08 to 480 ml/min. In cathode high purity of oxygen (99.99 %) was used as the oxidant and methanol molar concentrations (0.5 M, 1.0 M, 2.0 M and 3.0 M) were used as the anode fuel. The cathode reactant gas was conditioned to 30 °C and 100% relative humidity prior to entering the cell and methanol fed at the anode side at room temperature. The temperature given to the cell was measured by a thermocouple (K type) and the cell is heated using the heater plug

available on the test setup. The anode and cathode reactants were in **the** parallel flow without external back pressure.

A single cell consists of an MEA, anode and cathode flow channels (Graphite plate), gaskets, current collector plates (gold coated copper plate), end plates (Stainless steel), insulators and eight pairs of M6 nuts & bolts. The MEA was placed between anode and cathode flow channels and to improve sealing effect, a Teflon gasket of 0.2 mm thickness was kept between flow channel and MEA on both sides followed by the current collector plates for anode and cathode. An insulator material was kept between the current collector plate and endplate. The cell was assembled using eight bolts tightened to 4.2 Nm/bolt. The cell consisted of in-house machined graphite plates with a single pass serpentine flow field on both sides (anode and cathode flow channels) of 1 mm channel width-depth and 1:1 rib to channel ratio [13, 50]. **El-Zoheiry R. M [51] et.al, suggested that serpentine flow field designs enhancing the under-rib reactant mass transport to increase the efficiency of the fuel cell in terms of power density, and methanol utilization.** Since serpentine flow field is more stable and enhanced performance in DMFC due to its higher pressure drop, better reactant distribution and mass transport along **the** transverse direction in the flow channels [17,52]. Besides, 5 h short-term durability tests have been carried out for the anode electrode catalysts to assess their short term stability behaviours.

2.6 MEA conditioning

A number of experimental trails have been carried out for conditioning the MEA as well as to achieve enhanced proton conduction on the membrane from constant current and constant voltage modes. During conditioning, anode and cathode flow rates were set to 3 ml/min and 100 ml/min, respectively and cell temperature is maintained at 80 ℃. Conditioning of MEA (i.e, activation process) was conducted by applying voltage pulse. The following conditioning process gave the highest performances on the DMFCs examined in

this laboratory. Initially a constant cell voltage of 0.4 V was set for 20 minutes,then 0.2 V for the same duration. Next, cyclic looping process was conducted at constant voltage pulse for 20 cycles at 0.4 V and 0.2 V for 1 hour. This process ensures that, catalyst present in the active area was well activated.

3. Results and Discussion

3.1 Effect of anode catalysts

Investigations have been carried out to compare the performances of DMFCs assembled using conventional Pt/C cathode catayst and PtRu/C, Pt-$NiTiO_3$/C and Pt-Ru-$NiTiO_3$/C anode catalysts. Fig. 2 compares the performance of the Pt-$NiTiO_3$/C (anode) vs Pt/C (cathode) catalysts under optimum operating conditions of 80 ℃, 0.5 M methanol and 3 ml/min and 100 ml/min for anode and cathode flow rates. The selection criteria for operating parameters were made from the detailed studies described below which is used in all the performance tests. Additionally, conventional Pt/C vs Pt/C was tested in **the** same condition for comparison purpose. The MEA with Pt-$NiTiO_3$/C anode catalyst delivers the maximum power density of 13.3 mW/cm^2 and **the** maximum current density of 127 mA/cm^2, which is 45 % enhancement in power density when compared with commercial Pt/C (power density 7.3 mW/cm^2) as the anode catalyst**. The improvement in cell performance of Pt-$NiTiO_3$/C over Pt/C could be attributed to the synergetic effects of each component and also due to the increased methanol adsorption site. This observation is in agreement with the literature on Pt decorated with metal oxides promotes high stability and MOR activity by the synergetic effect [53].**

The reaction mechanism (1) of bifunctional electrocatalyst was proposed in our earlier work [37]. Due to the strong interaction between Pt and $NiTiO_3$ particles the MOR activity

was improved and the high power density of Pt-$NiTiO_3$/C shows high performance towards MOR.

$Pt\text{-}CO_{ads} + NiTiO_{3-x}(OH) \rightarrow Pt + NiTiO_{3-x} + CO_2 + H^+ + e^-$ (1)

The OH species from the aqueous electrolyte was absorbed by $NiTiO_3$ and supply to Pt for burning of CO species [41, 54]. The presence of $NiTiO_3$ helps to remove the CO poisoning species from the surface of Pt. It is interesting to note that Pt-$NiTiO_3$/C yields the peak power of 26.6 mW/mg_{Pt} from 5 cm^2 with a very low loading of platinum (0.5 mg_{Pt}/cm^2) which is several fold lesser compared to platinum loading reported for the electrocatalyst materials like PtRuMo/C (2 mg_{Pt}/cm^2) [55] and Pt$RuTiO_2$/C (4 mg_{Pt}/cm^2) [19]. Therefore, it is clear that $NiTiO_3$/C is acting as a promoter and helps in improving the poison tolerance of the electrocatalyst and thereby increasing the performance.

Fig. 3 compares the performances of the PtRu/C and Pt-Ru-$NiTiO_3$/C anode catalysts. Pt loading is maintained as 0.5 mg_{Pt}/cm^2 on both anode and cathode catalysts. Whilst the Pt-Ru-$NiTiO_3$/C catalyst showed a small drop in OCV from 0.57 V to 0.53 V compared to PtRu/C catalyst, the maximum current density and power density achieved by the Pt-Ru-$NiTiO_3$/C anode catalyst **is** 147 mA/cm^2 and 14.6 mW/cm^2 respectively. There is ~ 57 % enhancement in current density and ~ 22 % in power density when compared with PtRu/C (current density - 63 mA/cm^2 and power density - 11.4 mW/cm^2) respectively.

From the comparison, it is discernable that the higher power densities are obtained from the Pt-Ru-$NiTiO_3$/C, attributable to the presence of titante based metal oxides which helps to enhance the activity of Pt atoms for the adsorption and desorption reactions. In addition to that the catalyst contains **a** low amount of Ru-oxy hydroxide which does not play a major role and contribute to the high level of MOR enhanced activity [41]. The increased catalystic activity of the anode electrocatalyst shows the mixed synergitic effect of Ru and

$NiTiO_3$ and it helps to remove the CO_{ads} from the catalytic sites The reaction mechanism of Pt-Ru-$NiTiO_3$ electrocatalyst was also proposed in our earlier work [41] and shown below

$$Pt(CO_{ads}) + Ru\text{-}\ NiTiO_3(OH^-)_{ads} \rightarrow CO_2 + Pt + Ru + NiTiO_3 + H^+ + e^- \qquad (2)$$

In Table 1, the performances of the DMFCs fabricated with different anode catalysts and commercial Pt/C cathode catalyst are compared. Active geometrical area of the cells, type of membranes used, Pt loading levels at the anodes, peak power density values and peak power output (mW/mg_{Pt}) values of the DMFCs are compiled in this table. Peak power output (mW/mg_{Pt}) for various anode catslysts have been deduced by dividing the peak power density values by the Pt loading values. A comparison of the state of art of the performances of different catalysts suggests that our in house synthesized Pt-Ru-$NiTiO_3$/C and Pt-$NiTiO_3$/C catalysts show better performances of 29.2mW/mg_{Pt} and 26.6 mW/mg_{Pt} at the optimum operating conditions (80 ^oC, 0.5 M methanol, 3 ml/min), even with the low platinum loading of 0.5 mg_{Pt}/cm^2. It is found that our inhouse catalysts show enhanced performances compared to Pt$RuTiO_2$/C (17.6 mW/mg_{Pt}) [19], PtRuMo/C (24.5 mW/mg_{Pt}) [55] and performances comparable to that of PtRuMo/CNT (30.7 mW/mg_{Pt}) [56]. The variation in the performances is due to **the** synthesis method **[57],** higher loading of Pt on **the** cathode and various operating parametres.

3.2 Effect of cell operating temperature

The effect of operating parametres on the performance of the DMFCs has been examined for Pt-$NiTiO_3$/C (anode) and commercial Pt/C (cathode) catalysts. It can be noted in an earlier section that the variation in the peak power performances between Pt-$NiTiO_3$/C and Pt-Ru-$NiTiO_3$/C is minimum, while at the same time our previous studies [37,41] ensured titante based metal oxides play a significant effect on enhanced performance. Hence Pt$NiTiO_3$/C material only has been considered for further studies. Operating temperature plays a major role in activation of fuel cell electrodes and crossover of methanol [58, 59].

Jung et al. [60, 61] studied and reported that, increasing the cell temperature will significantly increase the performance of the DMFCs and decrease the activation loss and ohmic polarization loss which increase the electrochemical reaction rate faster. **At some point of futher increase in cell temperature will also increase the methanol cross over by Lee J et. al [15]**. Experiments were carried out, by using Pt-$NiTiO_3$ as the anode catalyst and the commercial Pt/C as the cathode catalyst with different operating temperatures of 45 ℃, 60 ℃ and 80 ℃. The results are shown in Fig.4.

It can be seen that the performance of the DMFCs with Pt-$NiTiO_3$/C catalyst improves with **the** temperature at 80 °C. The enhanced MOR kinetics yields better performance and it demonstrates that proposed cataylsts are thermally stable at the higher operating temperatures of 80 ℃. The maximum power densities attained at various temperatures are 9.6 mW/cm^2, 10.5 mW/cm^2 and 13.3 mW/cm^2 at 40 °C, 60 °C and 80 ℃ respectively. The mass transport of methanol is more **at a** higher temperature, since the diffusion rate of methanol will be higher. The performances of the DMFCs at higher temperature (80 ℃) are enhance not only due to higher methanol mass transfer but also due to enhanced electrochemical reaction rate, reduced water flooding and methanol crossover. The increased temperature also lowers cell resistance (reduces the ohmic loss) and decreases the activation loss. However, **a** further increment in temperature beyond 80 ℃, causes methanol crossover, degradation of **the** membrane by dehydration process [62], and catalyst degradation [63], and eventually the cell performance will be reduced.

3.3 Effect of methanol concentration

The concentration of methanol is also one of the parameters that affects the performance [64]. Eventhough higher methanol concentrations are beneficial in increasing the MOR activity in **the** anode, the problems of crossover of methanol will be more [65] and it may degrade the catalysts and their performances. **Yu B et al [66] also investigated the**

effect of methanol concentration ranging from 0.5 M to 1.0 M. The results suggests that increase in methanol concentration will also increase the methanol crossover thus leading to decrease in cell performance. Hence, the effect of methanol concentration on the performances of Pt-$NiTiO_3$/C catalyst has been examined by employing different methanol/water molar concentration (0.5 M, 1.0 M, 2.0 M, and 3.0 M) with **a** constant temperature of 80 ℃ with a view to determine the optimum concentration that will give maximum performance.

Fig.5 shows that as the methanol molar concentration increases from 0.5 M to 3.0 M, peak power density is reduced from 13.3 mW/cm^2 to 7.3 mW/cm². The results suggest that 0.5 M concentration is the optimum concentration that is required for the effective operation of the DMFCs. The catalyst activity at the anode gets restricted when the methanol concentration is increased and the surplus methanol will increase the methanol crossover from anode to cathode and reduces the cell performance. The higher methanol concentration will enhance the methonal crossover from anode to cathode, which reduces the methonal utilization. Also, open circuit voltage (OCV) has reduced due to mixed potential. The transfer rate of methanol from **the** anode flow channel to the catalyst layer is increased when methanol concentration increases from 0.5 M to 3 M and the diffusion force is higher due to the higher gradients.

3.4 Effect of anode flow rate

To investigate the influence of anode stoichiometry on performance, polarization curves were obtained at 1.0, 2.0, 3.0 and 4.0 ml/min anode flow rate, 0.5 M methanol concentration and 100 ml/min cathode flow rate. The results, shown in Fig.6, indicates that **the** maximum power density of 13.3 mW/cm^2 is obtained at 3 ml/min flow rate and it is due to the maximum diffusion rate of methanol. At the lowest flow rate of 1.0 ml/min, the performance of the DMFC is reduced due to the concentration loss caused by insufficient

supply of methanol and at the region of high current density it is in **an** electrically unstable state. This clearly suggests that the methanol crossover is very low. At the highest flow rate of 4.0 ml/min, 14.2 % drop in maximum power density performances from 13.3 mW/cm^2 has occurred and it is due to the increase of methanol crossover at an anode flow rate above 3 mL/min. This indicates that the methanol crossover is increased as the anode flow rate is increased and the excess methanol is not completely consumed due to **lower** reaction rate.

4. Stability test

The performance of a DMFC in real time is dependent on its ability to operate at a constant power or current over fixed voltage for a particular period of time. This characterization evaluation is known as the stability test. To evaluate the stabilities of the DMFCs based on PtRu/C and Pt-$NiTiO_3$/C as anode electrocatalysts, the following parameters were considered: cell temperature (80 ^oC), methanol molar concentration (0.5 M), anode flow rate (3 ml/min), cathode flow rate (100 ml/min) and the experimentation was conducted at 0.2 V for duration of 5 hours.

From the Fig. 7, it can be visualized that Pt-$NiTiO_3$ shows higher stability during the 5 hour experimentation. Moreover there is a negligible decline in power while Pt-$NiTiO_3$ is used as the catalyst. As mentioned earlier, this is due to the efficient conversion of CO to CO_2 by $NiTiO_3$ and high proton transfer rate facilitated by Ni. The DMFC yielded a steady power density in the range of 12.5 to 13 mW/cm^2 (62.5 to 65 mW) for the entire period of operation. The power density of the DMFC assembled with the Pt-$NiTiO_3$/C electrocatalyst is considerably higher than with PtRu/C over the entire period of time, indicating a higher stability during the reaction. Initial drop in the stability curve is noticed and it is because of the occurrence of insufficient diffusion **of methanol and oxygen [67]**. However, intermittent minor fluctuations are noticed in the stability curve and these fluctuations could be attributed to the following reasons: cathode water formation **[68],** methanol crossover **[21],** reduced

oxygen reduction reaction (ORR) **sluggish** kinetics at the cathode **[69]** and CO formation on **the** anode **[60].** Similar to PEMFC's, DMFC's too are influenced by the water formation along the cathode, which is the major cause for reduction in power over a period of time.

5. Conclusions

In this work, the performances of the DMFCs assembled with four different anode electrocatalyst materials (Pt/C, Pt-$NiTiO_3$/C, PtRu/C and Pt-Ru-$NiTiO_3$/C) were investigated. The performances tests were conducted with different cell operating temperatures (45 ℃, 60 ℃ and 80 ℃), methanol molar concentration (0.5 M, 1 M, 2 M and 3 M) and flow rates (1 ml/min, 2 ml/min, 3 ml/min and 4 ml/min). Investigations concluded that, at 0.5 M concentration of methanol, 3 ml/min of flow rate and 80 ℃ highest performances are obtained. The main conclusions derived from the experimental results are listed as follows.

- The Pt-$NiTiO_3$/C electrocatalyst has shown almost twice the performance (a power output of 26.6 mW/mg_{pt}) as that of the conventional Pt/C for 5 cm^2 active area with low loading of Pt (0.5 mg_{Pt}/cm^2). Similarly, Pt-Ru-$NiTiO_3$/C anode electrocatalys has given 22 % higher power output than that of the PtRu/C catalyst. This is due do the presence of strong interaction between Pt, Pt-Ru and $NiTiO_3$, and these interactions promotes the DMFC performances.
- $NiTiO_3$ promoted catalysts are promosing in increasing the stability for DMFCs.
- The hierarchy of order of performance of anode electrocatalysts are Pt/C < PtRu/C < Pt-$NiTiO_3$/C < Pt-Ru-$NiTiO_3$/C.

The overall results suggest that, **the** presence of $NiTiO_3$/C supportive material increase DMFC performances when Ru is combined with Pt even in the presence of lower Pt loading (0.5 mg_{Pt}/cm^2). This supportive material will pave way for achieving an improved performance for low cost and low power density DMFC applications.

Acknowledgements

We gratefully acknowledge DST-UKIERI (DST/INT/UK/P121/2016), India and Loughborough University, U.K for the financial support. The support and the facilities provided by the PSG management and PSG Insitute of Advanced Studies are acknowledged. The helps rendered by Dr. A. Sukana Nazerin, Mr. V. Rajavel, Mr. Alex Thirkell and Mr. C. Mathan are also appreciated.

Reference

1. Smitha B, Sridhar S, Khan AA. Solid polymer electrolyte membranes for fuel cell applications - A review. J Membr Sci 2005;259:10-26.
2. Faghri A, Li X, Bahrami H. Recent advances in passive and semi-passive direct methanol fuel cells. Int J Thermal Sciences 2012;62:12-18.
3. Ong BC, Kamarudin SK, Masdar MS, Hasran UA. Applications of graphene nano-sheets as anode diffusion layers in passive direct methanol fuel cells (DMFC). Int J Hydrogen Energy 2017;42:9252-9261.
4. Falcao DS, Pereira JP, Rangel CM, Pinto AMFR. Development and performance analysis of a metallic passive micro-direct methanol fuel cell for portable applications. Int J Hydrogen Energy 2015;40: 5408-5415.
5. Hampson NA, Wilars MJ. The methanol-air fuel cell: a selective review of methanol oxidation mechanisms at platinum electrodes in acid electrolytes. J Power Sources 1979;4:191-201.
6. Du CY, Zhao TS, Yang WW. Effect of methanol crossover on the cathode behavior of a DMFC: A half-cell investigation. Electrochim Acta 2007;52:5266-5271.
7. Hamnett A, in: Wieckowski A (Ed.). Interfacial Electrochemistry Theory, Experiment, and Applications. Marcel Dekker, New York, 1999 (Chapter 47).
8. Akhairi MAF, Kamarudin SK. Catalysts in direct ethanol fuel cell (DEFC): an overview. Int J Hydrogen Energy 2016;41:4214-4228.
9. Lee K, Nam JD. Optimum ionic conductivity and diffusion coefficient of ion-exchange membranes at high methanol feed concentrations in a direct methanol fuel cell. J Power Sources 2006;157:201-206.
10. Pan YH. Direct methanol fuel cell with concentrated solutions. Electrochem Solid-State Lett 2006;9:A349-351.

11. Shukla S, Stanier D, Saha MS, Stumper J, Secanell M. Analysis of inkjet printed PEFC electrodes with varying platinum loading. J Electrochem Soc 2016;163:F677-687.
12. Oliveira VB, Rangel CM, Pinto AMFR. Modelling and experimental studies on a Direct Methanol Fuel Cell working under low methanol crossover and high methanol concentrations. Int J Hydrogen Energy 2009;34:6443-6451.
13. Mullai Sudaroli B, Kumar Kolar A. Experimental and Numerical Study of Serpentine Flow Fields for Improving Direct Methanol Fuel Cell Performance. Fuel Cells 2015;15:826-838.
14. Gwak G, Kim D, Lee S, Ju H. Studies of the methanol crossover and cell performance behaviors of high temperature-direct methanol fuel cells (HT-DMFCs). Int J Hydrogen Energy 2018;43:13999-14011.
15. Lee J, Lee S, Han D, Gwak G, Ju H. Numerical modeling and simulations of active direct methanol fuel cell (DMFC) systems under various ambient temperatures and operating conditions. Int J Hydrogen Energy 2017;42:1736-1750.
16. García-Salaberri PA, Vera M. On the effects of assembly compression on the performance of liquid-feed DMFCs under methanol-limiting conditions: A 2D numerical study. J Power Sources 2015;285:543-558.
17. Nicolò S Vasile, Alessandro HA Monteverde Videla, Simari C, Nicotera I, Specchia S. Influence of membrane-type and flow field design on methanol crossover on a single-cell DMFC: An experimental and multi-physics modeling study. Int J Hydrogen Energy 2017;42:27995-28010.
18. Kamarudin SK, Hashim N. Materials, morphologies and structures of MEAs in DMFCs. Renewable and Sustainable Energy Reviews 2012;16:2494-2515.

19. Ercelik M, Ozden A, Seker E, Ozgur Colpan C. Characterization and performance evaluation of Pt-Ru/C-TiO_2 anode electrocatalyst for DMFC applications. Int J Hydrogen Energy 2017;42: 21518-21529.
20. Fathirad F, Mostafavi A, Afzali D. Bimetallic Pd-Mo nanoalloys supported on Vulcan XC-72R carbon as anode catalysts for direct alcohol fuel cell. Int J Hydrogen Energy 2017;42:3215-3221.
21. Sharma S, Pollet BG. Support materials for PEMFC and DMFC electrocatalysts-A review. J Power Sources 2012;208: 96-119.
22. Patel PP, Datta MK, Jampani PH, Hong D, Poston JA, Manivannan A, Kumta PN. High performance and durable nanostructured TiN supported Pt50–Ru50 anode catalyst for direct methanol fuel cell (DMFC). J Power Sources 2015;293:437-446.
23. Liu H, Song C, Zhang L, Zhang J, Wang H, Wilkinson DP. A review of anode catalysis in the direct methanol fuel cell. J Power Source 2006;155:95-110.
24. Antolini E, Platinum Alloys as Anode Catalysts for Direct Methanol Fuel Cells. In Electrocatalysis of Direct Methanol Fuel Cells: From Fundamentals to Applications (Wiley-VCH, Weinheim, 2009), 227–255.
25. Frelink T, Visscher W, van Veen JAR, On the role of Ru and Sn as promotors of methanol electro-oxidation over Pt. Surf Sci 1995;335:353-360.
26. Long JW, Stroud RM, Swider-Lyons KE, Rolison DR. How to make electrocatalysts more active for direct methanol oxidation - avoid PtRu bimetallic alloys! J Phys Chem B 2000;104:9772-9776.
27. Li Y, Bastakoti BP, Malgras V, Li C, Tang J, Kim JH, Yamauchi Y. Polymeric micelle assembly for the smart synthesis of mesoporous platinum nanospheres with tunable pore sizes. Angew Chem Int Ed 2015;54:11073-11077.

28. Li C, Yamaucni Y. Facile solution synthesis of Ag@Pt coreeshell Nanoparticles with dendritic Pt shells. Phys Chem Chem Phys 2013;15:3490-3496.
29. Mohan N, Cindrella L. Template-free synthesis of Pt-MOx (M¼ Ni, Co & Ce) supported on cubic zeolite-A and their catalytic role in methanol oxidation and oxygen reduction reactions characterized by the hydrodynamic study. Int J Hydrogen Energy 2017;42:21719-21731.
30. Abdelkareem MA, Ito Y, Tsujiguchi T, Nakagawa N. Carbon- TiO_2 composite nanofibers as a promising support for PtRu anode catalyst of DMFC. ECS Trans 2013;50:1959-1967.
31. Shan CC, Tsai DS, Huang YS, Jian SH, Cheng CL. Pt-Ir-IrO_2NT thin-wall electrocatalysts derived from IrO_2 nanotubes and their catalytic activities in methanol oxidation. Chem Mater 2007;19:424-431.
32. Zhang Y, Zhang H, Ma Y, Cheng J, Zhong H, Song S, Ma H. A novel bifunctional electrocatalyst for unitized regenerative fuel cell. J Power Source 2010;195:142-145.
33. Scibioh MA, Kim SK, Cho EA, Lim TH, Hong SA, Ha HY. Pt-zohei$_2$/C anode catalyst for direct methanol fuel cells. Appl Catal B: Environ 2008;84:773-782.
34. Maiyalagan T, Khan FN. Electrochemical oxidation of methanol on Pt/V_2O_5-C composite catalysts. Catal Commun 2009;10:433-436.
35. Micoud F, Maillard F, Gourgaud A, Chatenet M. Unique CO tolerance of Pt-WO_x materials. Electrochem Commun 2009;11:651-654.
36. Justin P, Rao GR. Methanol oxidation on MoO_3 promoted Pt/C electrocatalyst. Int J Hydrogen Energy 2011;36:5875-5884.
37. Thiagarajan V, Manoharan R, Karthikeyan P, Nikhila E, Hernandez-Ramirez A, Rodriguez-Varela FJ. Pt nanoparticles supported on $NiTiO_3$/C as electrocatalyst towards high performance Methanol Oxidation Reaction. Int J Hydrogen Energy 2017;42:9795-9805.

38. Tian X, Wang L, Deng P, Chen Y, Xia BY. Research advances in unsupported Pt-based catalysts for electrochemical methanol oxidation. J Energy Chem 2017;26:1067-1076.
39. Macak JM, Barczuk PJ, Tsuchiya H, Nowakowska MZ, Ghicov A, Chojak M, et al. Self-organized nanotubular TiO_2 matrix as support for dispersed Pt/Ru nanoparticles: Enhancement of the electrocatalytic oxidation of methanol. Electrochem Commun 2005;7:1417-1422.
40. Kang DK, Noh CS, Kim NH, Cho SH, Sohn JM, Kim TJ, Park YK. Effect of transition metals (Ni, Sn and Mo) in Pt_5Ru_4M alloy ternary electrocatalyst on methanol electro-oxidation. Journal of Industrial and Engineering Chemistry 2010;16:385-389.
41. Thiagarajan V, Karthikeyan P, Manoharan R, Sampath S, Hernández-Ramírez A, Sánchez-Castro ME, Alonso-Lemus IL, Rodríguez-Varela FJ. Pt-Ru-$NiTiO_3$ Nanoparticles Dispersed on Vulcan as High Performance Electrocatalysts for the Methanol Oxidation Reaction (MOR). Electrocatalysis 2018;9:582-592.
42. Pollet BG, Goh JTE. The importance of ultrasonic parameters in the preparation of fuel cell catalyst inks. Electrochim Acta 2104;128:292–303
43. Pollet BG. Let's Not Ignore the Ultrasonic Effects on the Preparation of Fuel Cell Materials. Electrocatalysis 2014;5330-5343.
44. Bender G, Zawodzinski TA, Saab AP. Fabrication of high precision PEFC membrane electrode assemblies. J Power Sources 2003;124:114-117.
45. Chun YG, Kim CS, Peck DH, Shin DR. Performance of a polymer electrolyte membrane fuel cell with thin film catalyst electrodes. J Power Sources 1998;71:174-178.
46. Kim CS, Chun YG, Peck DH, Shin DR. A novel process to Fabricate Membrane Electrode Assemblies for Proton Exchange Membrane Fuel Cells. Int J Hydrogen Energy 1998;23:1045-1048.

47. Park IS, Li W, Manthiram A. Fabrication of catalyst-coated membrane-electrode assemblies by doctor blade method and their performance in fuel cells. J Power Sources 2010;195:7078-7082.
48. Glass DE, Olah GA, Prakash GKS. Effect of the thickness of the anode electrode catalyst layers on the performance in direct methanol fuel cells. J Power Sources 2017;352:165–173.
49. Chen C, Yang P. Performance of an air-breathing direct methanol fuel cell. J Power Sources 2003;123:37–42.
50. Karthikeyan P, Velmurugan P, George AJ, Ram Kumar R, Vasanth RJ. Experimental investigation on scaling and stacking up of proton exchange membrane fuel cells. Int J Hydrogen Energy 2014;39:1186-1195.
51. El-Zoheiry RM, Ookawara S, Ahmed M. Efficient fuel utilization by enhancing the under-rib mass transport using new serpentine flow field designs of direct methanol fuel cells. Energy Conversion and Management 2017;144:88–103.
52. Choi KS, Kim HM, Moon SM. Numerical studies on the geometrical characterization of serpentine flow-field for efficient PEMFC. Int J Hydrogen Energy 2011;36:1613-1627.
53. Liu F, Dang D, Tian X. Platinum-decorated three dimensional titanium copper nitride architectures with durable methanol oxidation reaction activity. Int J Hydrogen Energy 2019; https://doi.org/10.1016/j.ijhydene.2019.02.059.
54. Manoharan R, Prabhuram J. Possibilities of prevention of formation of poisoning species on direct methanol fuel cell anodes. J Power Sources 2001;96:220-225.
55. Tsiouvaras N, Martinez-Huerta MV, Paschos O, Stimming U, Fierro JLG, Pena MA. PtRuMo/C catalysts for direct methanol fuel cells: Effect of the pretreatment on the structural characteristics and methanol electrooxidation. Int J Hydrogen Energy 2010;35:11478-11488.

56. Chen S, Ye F, Lin W. Effect of operating conditions on the performance of a direct methanol fuel cell with PtRuMo/CNTs as anode catalyst. Int J Hydrogen Energy 2010;35:8225-8233.
57. Lin ML, Lo MY, Mou CY. PtRu Nanoparticles Supported on Ozone-Treated Mesoporous Carbon Thin Film as Highly Active Anode Materials for Direct Methanol Fuel Cells. J. Phys. Chem. C 2009;113:16158–16168.
58. Chu D, Jiang R. Effect of operating conditions on energy efficiency for a small passive direct methanol fuel cell. Electrochim Acta 2006;51:5829-5835.
59. Jiang R, Chu D. Comparative studies of methanol crossover and cell performance for a DMFC. J Electrochem Soc 2004;151:A69-76.
60. Jung GB, Su A, Tu CH, Weng FB. Effect of operating parameters on the DMFC performance. J Fuel Cell Sci Tech 2004;2:81-85.
61. Jung DH, Lee CH, Kim CS, Shin DR. Performance of a direct methanol polymer electrolyte fuel cell. J Power Sources 1998;71:169-173.
62. Devrim Y, Erkan S, Bac N, Eroglu I. Improvement of PEMFC performance with Nafion/inorganic nanocomposite membrane electrode assembly prepared by ultrasonic coating technique. Int J Hydrogen Energy 2012;37:16748-16758.
63. Yang C, Costamagna P, Srinivasan S, Benziger J, Bocarsly AB. Approaches and technical challenges to high temperature operation of proton exchange membrane fuel cells. J Power Sources 2001;103:1-9.
64. Oliveira VB, Rangel CM, Pinto AMFR. Water management in direct methanol fuel cells. Int J Hydrogen Energy 2009;34:8245-8256.
65. Garcia MF, Sieben JM, Pilla AS, Duarte MME, Mayer CE. Methanol/air fuel cells: catalytic aspects and experimental diagnostics. Int J Hydrogen Energy 2008;33:3517-3521.

66. Yu B, Yang Q, Kianimanesh A, Freiheit T, Park SS, Zhao H, Xue D. A CFD model with semi-empirical electrochemical relationships to study the influence of geometric and operating parameters on DMFC performance. Int J Hydrogen Energy 2013;38:9873–9885.
67. Chen CY, Tsao CS. Characterization of electrode structures and the related performance of direct methanol fuel cells. Int J Hydrogen Energy 2006;31:391-398.
68. Casalongue HS, Kaya S, Viswanathan V, Miller DJ, Friebel D, Hansen HA, Nørskov JK, Nilsson A, Ogasawara H, Direct observation of the oxygenated species during oxygen reduction on a platinum fuel cell cathode. Nat. Commun. 2013;4:2817.
69. Matsuoka K, Iriyama Y, Abe T, MatsuokaM, Ogumi Z. Electro-oxidation of methanol and ethylene glycol on platinum in alkaline solution: poisoning effects and product analysis. Electrochim. Acta 2005;51:1085-1090.

Table

Table. 1 - A comparison of the state of art of the performances of the DMFCs.

Catalyst	Active Area (geometrical)	Pt Loading Anode	Membrane	Peak Power Density (mW/cm^2)	Peak Power Output (mW/mg_{Pt})	References
PtRuMo/C	1.1 cm^2	2 mg_{pt}/cm^2	Nafion 117	49	24.5	**[55]**
PtRu/C	5 cm^2	2 mg_{pt}/cm^2	Nafion 115	55.2	27.6	**[56]**
PtRu/CNT				55.8	27.9	
PtRuMo/CNT				61.3	30.7	
$PtRuTiO_2$/C	25 cm^2	4 mg_{PtRu}/cm^2	Nafion 115	70.9	17.7	**[19]**
PtRu/C	25 cm^2	4 mg_{PtRu}/cm^2	Nafion 115	55.5	13.9	
Pt-$NiTiO_3$/C	5 cm^2	0.5 mg_{Pt}/cm^2	Nafion 117	13.3	26.6	Present Work
Pt-Ru-$NiTiO_3$/C				14.6	29.2	
Pt/C				7.3	14.6	
Pt-Ru/C				11.4	22.8	

Figure

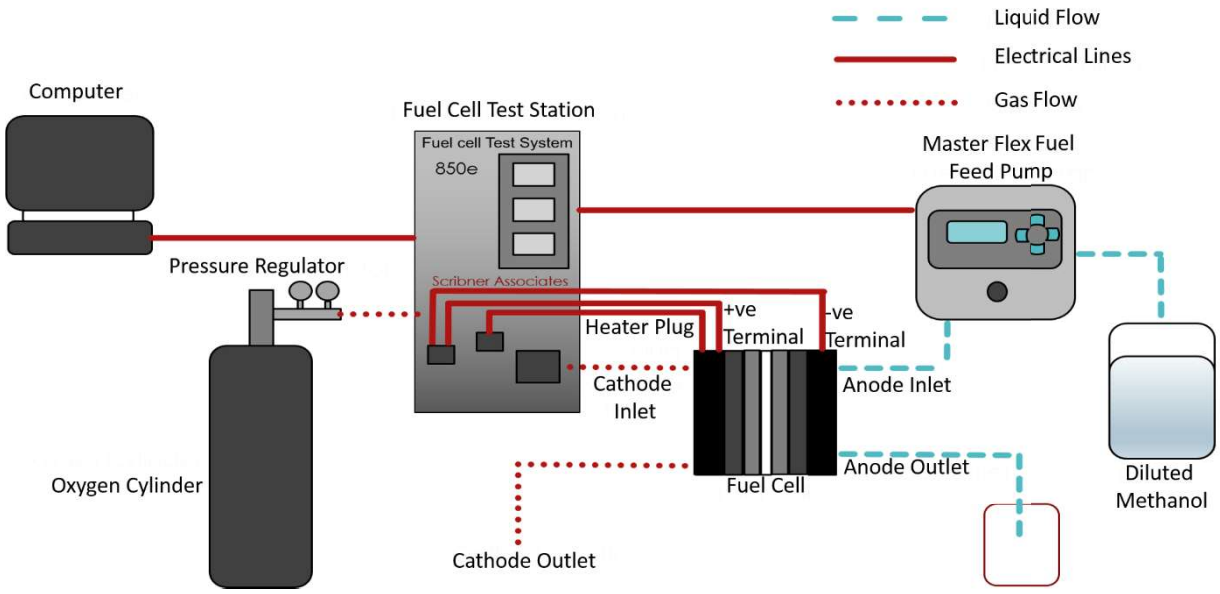

Fig.1 – Schematic diagram of DMFC test setup interfaced with Master Flex Peristaltic Pump

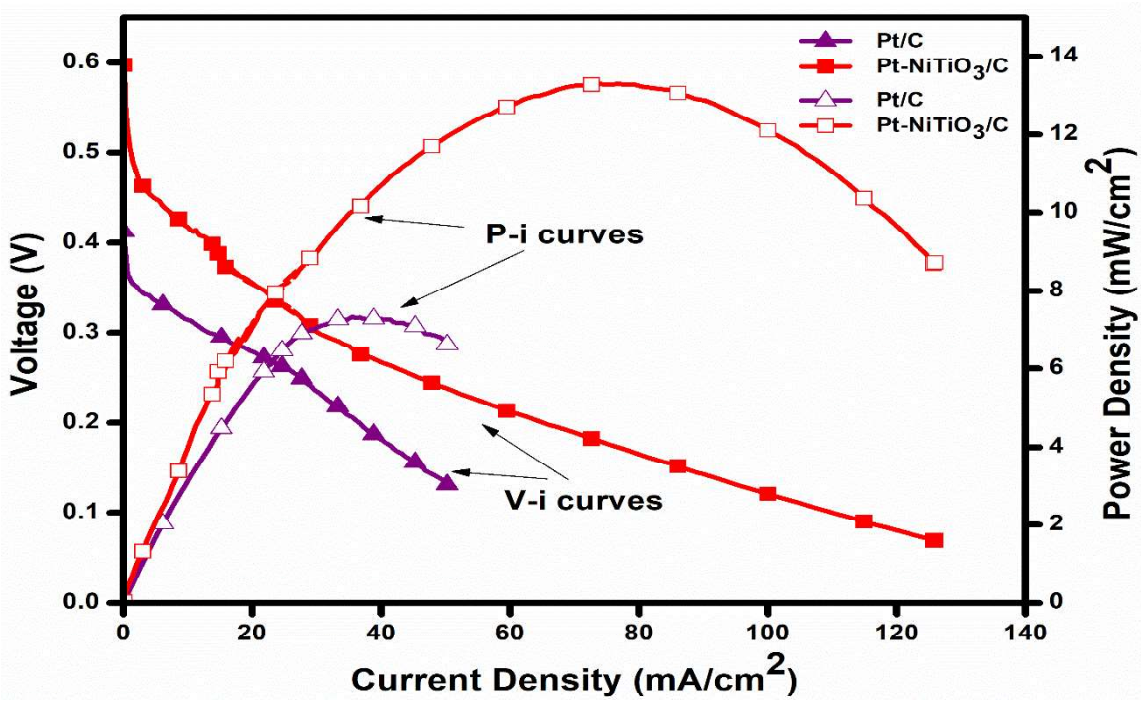

Fig. 2 - Polarization (V-i) and Power Density (P-i) curves of the DMFCs in comparison with different anode catalyst Pt/C and Pt-$NiTiO_3$/C.

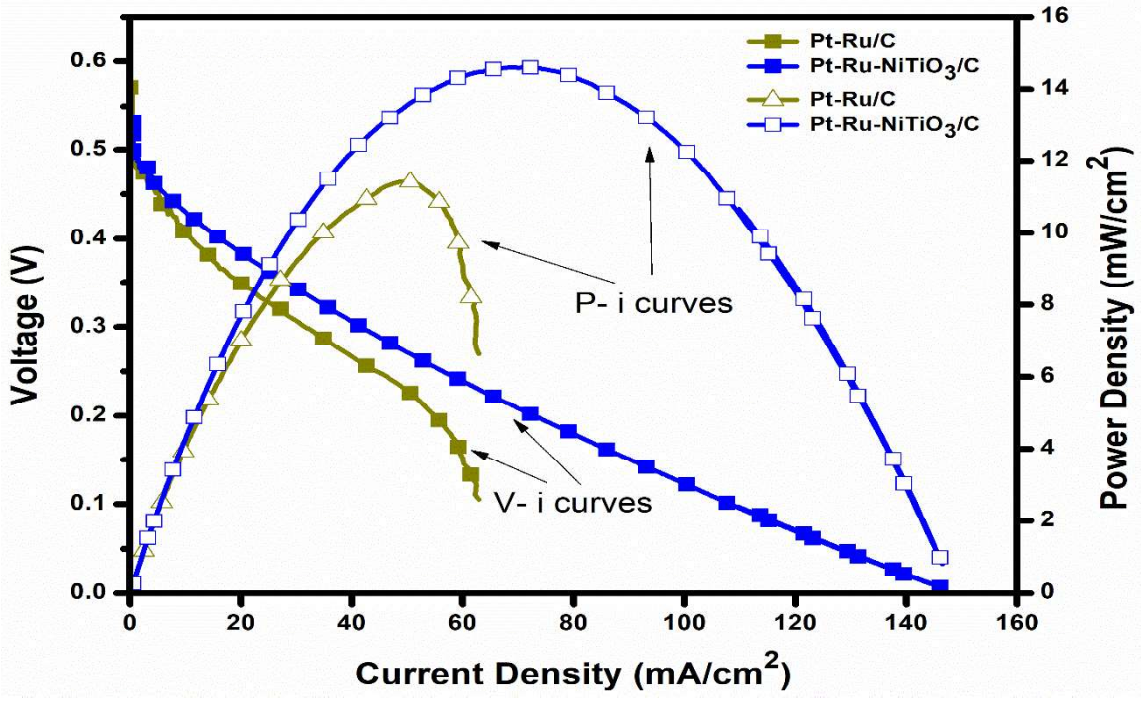

Fig. 3 - Polarization (V-i) and Power Density (P-i) curves of the DMFCs with different anode catalysts PtRu/C and Pt-Ru-$NiTiO_3$/C.

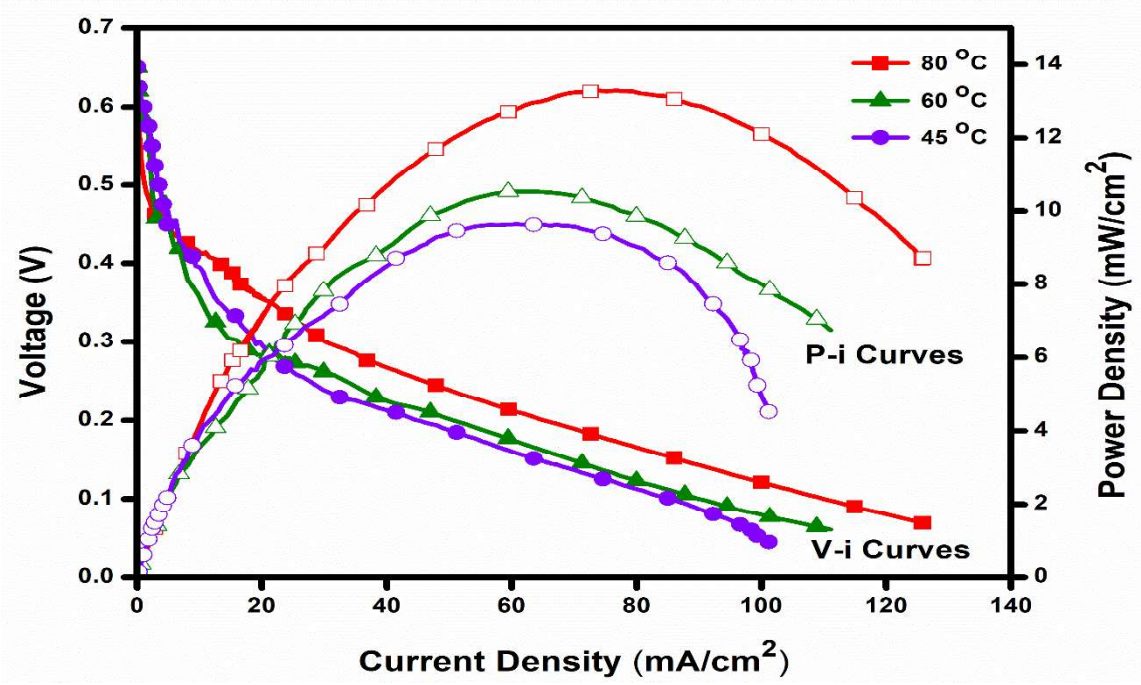

Fig. 4 - Polarization (V-i) and Power Density (P-i) curves of the DMFCs with 5 cm^2 active area for different operating temperature (45 °C, 60 °C and 80 °C).

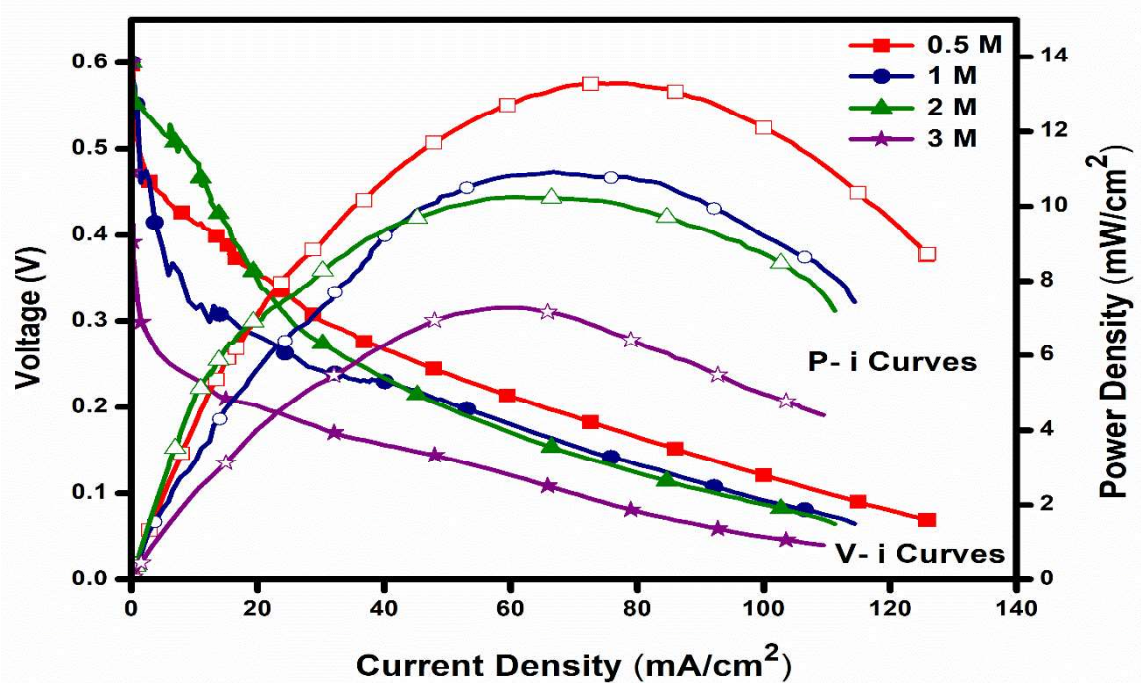

Fig. 5 - Polarization (V-i) and Power Density (P-i) curves of the DMFCs for different molar concentrations of methanol.

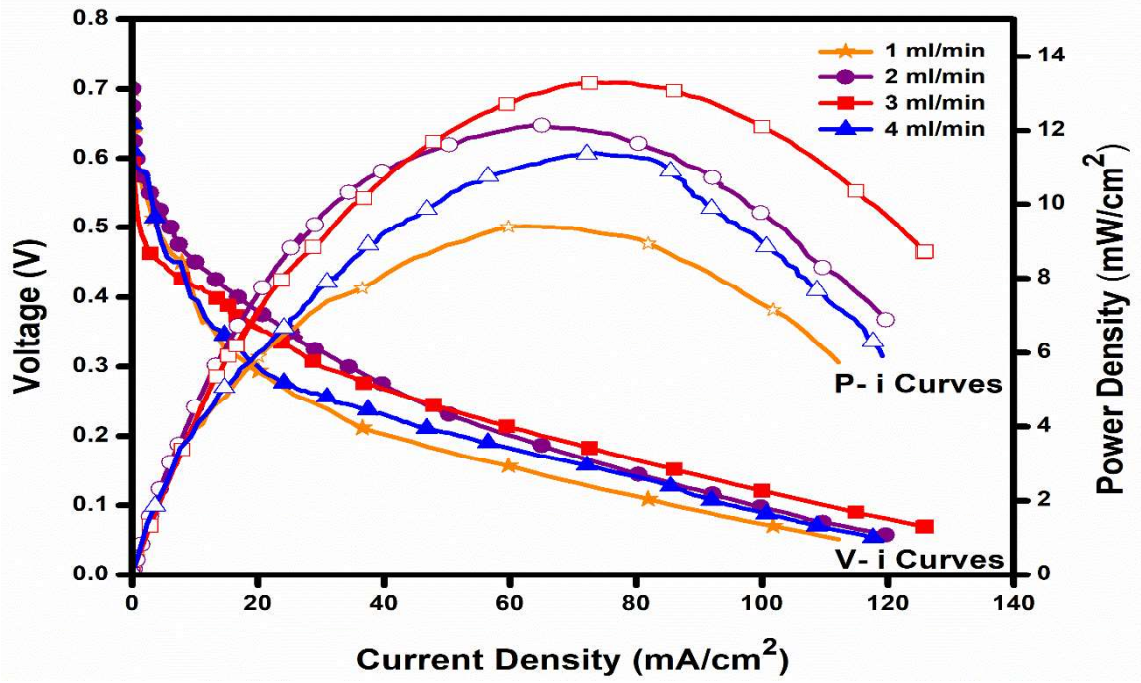

Fig. 6 - Polarization (V-i) and Power Density (P-i) curves of the DMFCs for different anode reactant flow rate.

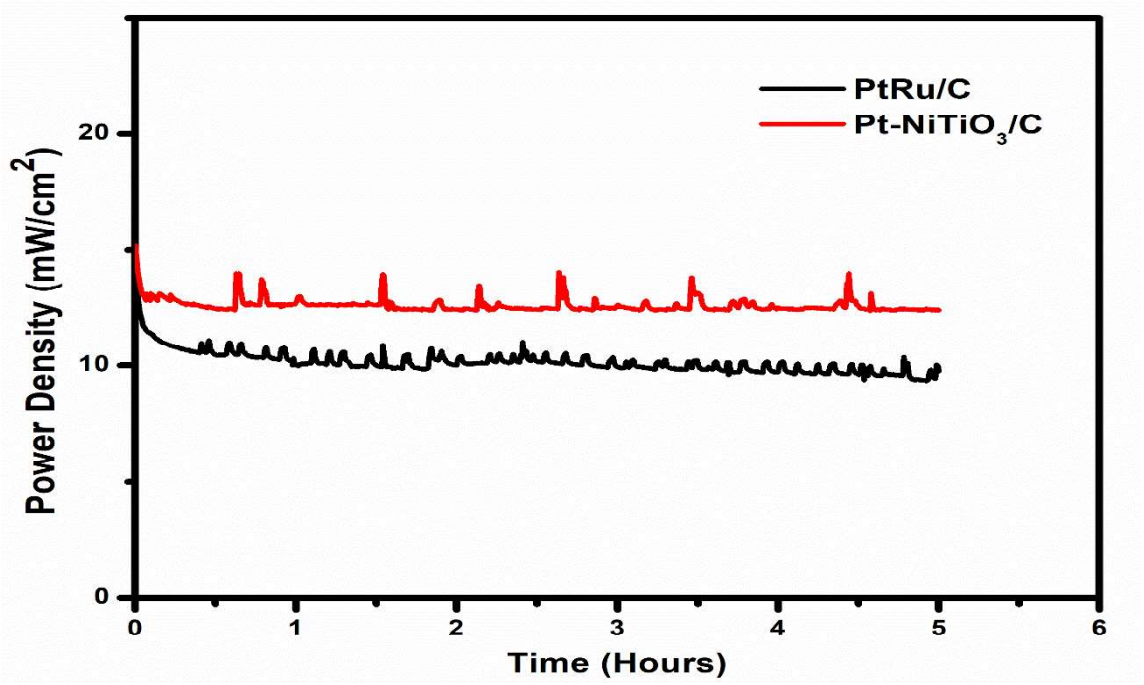

Fig. 7 - Short term durability test of DMFC based on in-house synthesized PtRu/C and Pt-$NiTiO_3$/C anode catalyst for 5 hours